In vivo analysis of human immune responses in immunodeficient rats.

Séverine Menoret, Laure-Hélène Ouisse, Laurent Tesson, Severine Remy, Claire Usal, Aude Guiffes, Vanessa Chenouard, Pierre-Joseph Royer, Gwénaëlle Evanno, Bernard Vanhove, et al.

Transplantation Publish Ahead of Print

DOI: 10.1097/TP.0000000000003047

In vivo analysis of human immune responses in immunodeficient rats.

Séverine Ménoret[1,2,3]*, Laure-Hélène Ouisse, PhD[1,2,3], Laurent Tesson[1,2,3], Séverine Remy, PhD[1,2,3], Claire Usal[1,2,3], Aude Guiffes[1,2,3], Vanessa Chenouard[1,2,3], Pierre-Joseph Royer, PhD[4], Gwenaelle Evanno[4], Bernard Vanhove, PhD[4], Eliane Piaggio, PhD[5], and Ignacio Anegon, MD, PhD[1,2,3]*.

[1] Centre de Recherche en Transplantation et Immunologie UMR1064, INSERM, Université de Nantes, Nantes, France.

[2] Institut de Transplantation Urologie Néphrologie (ITUN), CHU Nantes, Nantes, France.

[3] Nantes Université, CHU Nantes, Inserm, CNRS, SFR Santé, Inserm UMS 016, CNRS UMS 3556, F-44000 Nantes, France.

[4] Xenothera, Nantes, France.

[5] PSL Research University, Institut Curie Research Center, INSERM U932, Paris, France

* corresponding authors: Séverine Ménoret, CRTI, Nantes Université, CHU Nantes, Inserm, CNRS, SFR Santé, Inserm UMS 016, CNRS UMS 3556, 30 Bd Jean Monnet F-44093 Nantes, France. Email: severine.menoret@univ-nantes.fr

Ignacio Anegon, CRTI, Nantes Université, CHU Nantes, Inserm, CNRS, SFR Santé, Inserm UMS 016, CNRS UMS 3556, 30 Bd Jean Monnet F-44093 Nantes, France. Email: ianegon@nantes.inserm.fr

Authorship page

Séverine Ménoret. Designed and performed research, analyzed data and edited the manuscript.

Laure-Hélène Ouisse. Designed and performed research, analyzed data and edited the manuscript.

Laurent Tesson. Performed research and analyzed data.

Séverine Remy. Performed research and analyzed data.

Claire Usal. Performed research and analyzed data.

Aude Guiffes. Performed research and analyzed data.

Vanessa Chenouard. Performed research and analyzed data.

Pierre-Joseph Royer. Performed research and analyzed data.

Gwenaelle Evanno. Performed research and analyzed data.

Bernard Vanhove. Participated in provided reagents and edited manuscript

Eliane Piaggio. Provided reagents and edited manuscript.

Ignacio Anegon. Designed research, provided funding, analyzed data and wrote the manuscript.

Disclosure: Pierre-Joseph Royer, Gwenaelle Evanno and Bernard Vanhove are employees of Xenothera. The other authors declare no conflict of interest.

Funding. This work was performed in the context of different programs: Biogenouest by Région Pays de la Loire, IBiSA program, TEFOR (Investissements d'Avenir French Government program, ANRII-INSB-0014), LabCom SOURIRAT project (ANR-14-LAB5-0008), Labex IGO project (Investissements d'Avenir French Government program, ANR-11-LABX-0016-01), IHU-Cesti project (Investissements d'Avenir French Government program, ANR-10-IBHU-005, Nantes Métropole and Région Pays de la Loire) and Fondation Progreffe. TransImm team (E.P.) is supported by LabEx DCBIOL (ANR-10-IDEX-0001-02 PSL and ANR-11-LABX-0043), SIRIC INCa-DGOS-Inserm_12554, Center of Clinical Investigation (CIC IGR-Curie 1428).

Abstract.

Background. Humanized immune system immunodeficient mice have been extremely useful for the in vivo analyses of immune responses in a variety of models, including organ transplantation and GVHD but they have limitations. Rat models are interesting complementary alternatives presenting advantages over mice, such as their size and their active complement compartment. Immunodeficient rats have been generated but human immune responses have not yet been described.

Methods. We generated immunodeficient RRGS rats (for Rat Rag-/- Gamma chain-/- hSIRPa-positive) combining Rag1 and Il2rg deficiency with the expression of human SIRPalpha, a negative regulator of macrophage phagocytosis allowing repression of rat macrophages by human CD47-positive cells. We then immune humanized RRGS animals with human PBMCs to set up a human acute GVHD model. Treatment of GVHD was done with a new porcine anti-human lymphocyte serum (LIS1) active through complement-dependent cytotoxicity. We also established a tumor xenograft rejection model in these human PBMCs immune system RRGS animals by subcutaneous implantation of a human tumor cell line.

Results. RRGS animals receiving human PBMCs showed robust and reproducible reconstitution, mainly by T and B cells. A dose-dependent acute GVHD process was observed with progressive weight loss, tissue damage and death censoring. LIS1 antibody completely prevented acute GVHD. In the human tumor xenograft model, detectable tumors were rejected upon hPBMCs injection.

Conclusions. Human PBMC can be implanted in RRGS animals and elicit acute GVHD or rejection of human tumor cells and these are useful models to test new immunotherapies.

Abbreviations

67p. Pig purified IgG from nonimmunized animals.

ADCC. Antibody-dependent cytotoxicity

aGVHD. Acute graft-versus host disease

ALT. Alanine transaminase

AST. Aspartate transaminase

ATG. Anti-thymocyte globulin

BAC. Bacterial artificial chromosome

CDC. Complement-dependent cytotoxicity

FBS. Fetal bovine serum

hPBMC. Human peripheral blood mononuclear cells

Il2rg. IL-2 receptor gamma

Ip. Intraperitoneal

iv. Intravenous

LIS1. Pig purified IgG anti-human lymphocytes

LN. Lymph node

NOD. Nonobese diabetic mice

PKRDC. DNA-dependent protein kinase catalytic subunit

Rag1. Recombination activating gene 1

Rag2. Recombination activating gene 2

RRG. Rat Rag1-deficient, Il2rg-deficient

RRGS. Rat Rag1-deficient, Il2rg-deficient, hSIRPa+

Scid. Severe combined immunodeficient

SD/Crl. Sprague-Dawley from Charles River

SIRPa. Signal regulatory protein alpha

TALEN. Transcription activator-like effector nucleases

Introduction.

Immunodeficient mice in particular have been extremely useful for the analysis of in vivo functions and biological performances of different molecules that are immunogenic, and additionally, to humanize different tissues to generate a variety of human pathophysiological models.[1,2] Nevertheless, alternative models are needed since their small size is an obstacle for the development of different models. Furthermore, some inherent characteristics are also obstacles for other applications. For example, most mouse inbred strains show levels of complement much lower than those of rat and human sera.[3] Rats are a useful alternative since they are ten-fold bigger than mice allowing more frequent blood sampling and in larger volumes, to harvest larger number of cells and to perform surgical procedures, such as implantation of cells into organs such as the brain, prostate or ovaries. Furthermore, in some models, rats have proven to better reproduce pathologies observed in humans, such as Duchenne disease following gene inactivation of dystrophin[4] and in these models availability of immunodeficient rats would be very useful to test treatments such as human stem cells or gene therapy without the interference of immune responses. Finally, there are some immunological similarities between rats and humans that are not presented in mice. For example, activated T cells in humans and rats, but not in mice, express MHC class II and FoxP3 molecules and expression of CD8 and CD4 are detected on human and rat, but not mouse macrophages.[5]

Immunodeficient rats with single or combined deficiencies in genes involved in immune adaptive immune responses, such as *Prkdc, Rag1, Rag2* and *Il2rg,* have been described.[6-10] These rats, although capable of accepting certain human tissues, such as tumors and skin grafts, were refractory to humanization using isolated human cells, such as CD34+ hematopoietic precursors or peripheral blood mononuclear cells (PBMCs) and showed low efficacy of liver humanization with hepatocytes.[6,8,10]

In mice immunodeficient for the genes mentioned above hematopoietic or liver humanization were also inefficient. These humanizations are prevented by a molecular incompatibility between mouse macrophage SIRPalpha and human CD47 expressed on all hematopoietic cells, that normally provide "don't eat me" signals. Humanization was greatly ameliorated in immunodeficient mice in which SIRPa/human CD47 interaction was restored.[1,2,11,12] The finding that the mouse NOD strain has a spontaneous mutation that allows mouse macrophage SIRPalpha and human CD47 interactions explained the better humanization obtained with this strain.[13] However, the NOD strain has also genetic deficiencies in the complement system[14] and lack NK cells.[15] These are obstacles for its use in the evaluation of antibody effector functions such as complement-dependent cytotoxicity (CDC) and antibody-dependent cellular cytotoxicity (ADCC). Other mouse strains, such as C57/Bl6, were genetically modified to introduce human SIRPalpha (hSIRPa) in macrophages[11] but nevertheless, all inbred mouse strains including C57/Bl6 show much lower levels of complement as compared to human or rat serum.[3]

A recent publication described immunodeficient rats expressing hSIRPa that were immune humanized but analyses of human immune responses were not reported.[16] To obtain humanization of the immune system using PBMCs in rats and then analyze immune responses, we crossed rats that are deficient for *Rag1* and *Il2rg* (RRG animals)[10] with a transgenic rat line expressing human hSIRPa in rat macrophages[17] to obtain RRGS animals. We show that RRGS animals present efficient, robust and reproducible humanization of immune cells using PBMCs, with the development of acute graft-versus host disease (aGVHD) if sufficient numbers of hPBMCs were injected. GVHD could be inhibited by treatment with a new anti-human lymphocyte polyclonal antibody produced in pigs, mainly functioning through complement-mediated cytotoxicity. We also describe an efficient human immune response against human tumor cells in PBMC-humanized RRGS animals. In summary, we established for the first time a robust human immune response in immunodeficient rats.

Materials and Methods.

Animals.

Rats deficient for *Rag1*$^{-/-}$ and *Il2rg*$^{-/-}$ (RRG) generated using meganucleases and TALENs[10] and h*SIRPa* transgenic rats generated using a human BAC with promoter sequences[17] have been previously described and were crossed to obtain RRGS rats that were maintained under specific pathogen-free conditions. Rats were genotyped using microcapillary electrophoresis as previously described.[18] Wild type Sprague-Dawley (SD/Crl) rats were from Charles River (L'Arbresle, France). All animal care and procedures performed in this study were approved by the Animal Experimentation Ethics Committee of the Pays de la Loire region, France, in accordance with the guidelines from the French National Research Council for the Care and Use of Laboratory Animals (Permit Numbers: Apafis 692, Apafis 17305 and Apafis 17306). All efforts were made to minimize suffering. The rats were housed in a controlled environment (temperature 21±1°C, 12-h light/dark cycle).

Cytofluorimetry and antibodies.

Single-cell suspensions from the spleen, thymus, bone marrow and lymph nodes were prepared as described previously.[19] Cell suspensions were analyzed using FITC-conjugated mouse anti-rat CD3 (clone G4.18) and FITC-conjugated mouse anti-rat TCRαβ. Allophycocyanin (APC)-conjugated mouse anti-rat IgD (clone MARD-3) was obtained from AbD Serotec (Oxford, UK). FITC-conjugated mouse anti-rat IgM μ chain was bought from Jackson ImmunoResearch Laboratories (West Grove, PA, USA). APC-conjugated mouse anti-rat CD161 (clone 3.2.3), phycoerythrin (PE)-conjugated mouse anti-rat CD45R (rat B220; clone His 24), PE-conjugated mouse anti-rat CD4 (clone OX35), and APC-conjugated mouse anti-rat CD8 (clone OX8) were from AbD (Serotec), and FITC-conjugated mouse anti-rat CD172a (clone OX41). PE-conjugated anti-human SIRPA monoclonal antibody (clone REA144, Miltenyi), Recombinant human CD47-Fc (hCD47-Fc, R&D Systems), PE-Cy7-conjugated anti-human CD45 (clone H130, BD Biosciences), PE-conjugated anti-human CD3 (clone HIT3a, BD Biosciences),

APC-conjugated anti-human CD56 (clone HCD56, Biolegend), Pacific Blue-conjugated anti-human CD14 (clone M5E2, BD Biosciences) and FITC-conjugated anti-human CD19 (clone HIB19, BD Biosciences).

The incubation period was 30 min at 4°C, and the analysis was performed with a FACSVerse system (BD Biosciences, Franklin Lakes, NJ) and FlowJo software (Tree Star, Ashland, OR).

Immune humanization using human PBMCs (hPBMCs).

hPBMCs from healthy volunteers were isolated from buffy coat preparations using Ficoll-Hypaque density gradients and freshly injected iv into 3-4-week-old RRG or RRGS animals (210-350 g). PBMCs were injected in different numbers depending on the model as indicated in the respective sections.

Treatment with liposomes containing clodronate.

Clodronate liposomes were purchased from Liposoma B.V. (Netherlands; www.clodronateliposomes.org) and prepared as recommended.[20] Briefly, rats were weighed, and 10 ml/kg of suspended solution was administered i.p. twice a week.

Generation of a new anti-human lymphocyte polyclonal antibody produced in pigs.

LIS1 (Low Immunogenicity Anti Lymphocyte Serum) is a swine polyclonal IgG anti-human T lymphocyte, devoid of specific sialic acid N-Glycolylneuraminic acid and α1-3 galactose carbohydrate xenoantigens to reduce the potential for adverse events such as serum sickness disease and allergy. It was generated by Xenothera (Nantes, France) by immunization of genetically modified pigs deficient for CMP-*N*-acetylneuraminic *acid* hydroxylase and in α1-3 galactosiltransferase enzymes with cells derived from a human leukemia T cell line. LIS1 was purified from serum by affinity and ion exchange chromatography steps and formulated in physiological buffer containing polysorbate 80.

In vitro complement-mediated cytotoxicity (CDC) against human PBMCs with LIS1.

Human PBMCs were isolated from 3 healthy donors by Ficoll (Eurobio, France) density gradient centrifugation. $2.5.10^5$ PBMC were incubated with increasing doses of purified pig LIS1 IgG antibodies or control nonimmune (67p) IgG in PBS 1% BSA (Merck, France) for 30 min at 4°C. PBMC were then washed twice with PBS 1% BSA and resuspended on ice in 25µl of neat human, mouse or rat serum. After 30 min incubation at 37°C, PBMC were washed twice with PBS 1% BSA on ice and resuspended in 100µl of propidium iodide at 4µg/ml (Merck, France). Cell cytotoxicity was determined by the % of PI positive cells on a Canto II flow cytometer (BD Biosciences, Franklin Lakes, NJ).

aGVHD model and treatment with LIS1. Rats were injected iv with human PBMCs (430.10^6 cells/kg). Acute GVHD clinical evaluation included weight loss, physical activity, hutch posture, skin lesions, diarrhea and fur texture that generated a clinical score (for each no=0; yes=1). Analyses of alanine and aspartate transaminases (AST and ALT, respectively) were performed in sera using standard biochemical assays.

For evaluation of LIS1 activity, rats were injected iv with PBMCs (215.10^6 cells/kg) and ip with LIS1 or control nonimmune pig IgG (67p) at 40 mg/kg at day 0 and biweekly during 28 days.

B2 breast cancer cell line.

This cell line was generated from a fresh sample of a metastatic lymph node (LN) from a breast cancer patient without neoadjuvant chemotherapy, undergoing primary partial mastectomy with axillary lymph node dissection at Institut Curie Hospital (Paris, France) in accordance with institutional ethical guidelines. Clinico-pathological characteristics of the tumor were: invasive breast carcinoma of no specific type, estrogen receptor positive, progesterone receptor positive, HER2 negative and grade 3 tumor with a Ki67 of 45%. The LN sample was cut into small fragments, digested with 0.1 mg/ml Liberase TL (Merck, France) in the presence of 0.1 mg/ml DNase (Merck, France) for 30 min in CO2 independent medium. Cells were filtered on

a 40-µm cell strainer (BD Biosciences) and washed. Cells were stained with PERCP-e710 anti-EPCAM (Thermofischer Scientific, France) and APC-Cy7 anti-CD45 (BD) and Dapi. Tumor cells were isolated as EPCAM (+) CD45(-) by cell sorting on a FACSAria instrument (BD Biosciences). Cells were grown in RPMI 1640 10% bovine serum (Thermofischer Scientific, France) in a 48 well plate. Cells were characterized by ploidy evaluation by cytofluorometry analysis, comparative genomic hybridization and immunochemistry.

Immune responses against human tumor cells.

Human mammal cancer cells from line B2 (15.10^6 cells) were injected subcutaneously in 12-week-old RRGS animals. Human PBMCs (161.10^6 cells/kg) were injected iv when tumors were palpable. Tumors were measured every 2-3 days (length [a] and width [b]) in millimeters using calipers, and tumor volumes (V) were calculated using the formula V = ab2/2, where a is the longer of the 2 measurements.

Statistical analysis

Results are presented as means ± SD. Statistical analysis between samples was performed by a Mann-Whitney test and for graft survival by a Kaplan-Meier test, using GraphPad Prism 4 software (GraphPad Software, San Diego, CA, USA). Differences associated with probability values of ^{a} $P<0.05$, ^{b} $P<0.005$, ^{c} $P<0.0002$ and $^{d}<0.0001$ were considered statistically significant.

Results.

Generation and characterization of RRGS animals.

Cytofluorimetric analysis of immune cells in the spleen **(Fig 1A-B)** and bone marrow **(Fig 1C)** of RRGS animals showed absence of mature T, B and NK cells. Identical phenotype was also already reported for RRG animals.[10] Lymph nodes were severely atrophic due to the absence of lymphoid development, as it is observed in immunodeficient mice[1,2] and RRG animals[10] and were not analyzed for cell composition.

A large majority of $CD11b^+$ cells (among mononuclear cells only monocytes/macrophages due to the absence of NK cells) from spleen from RRGS were $hSIRPa^+$ and all of these cells were also rat $SIRPa^+$ **(Fig. 1 D and E)**. Furthermore, $hSIRPa^+$ monocyte/macrophages showed specific binding of human CD47, one of the ligands of SIRPa, whereas rat SIRPa+ macrophages from WT animals did not **(Fig. 1 D and E)**.

Thus, RRGS have a profound immunodeficient phenotype for T, B and NK compartments and all rat macrophages express a functional hSIRPa, in accordance with the genomic regulatory sequences of hSIRPa present in hSIRPa transgenic rats (Jung, Menoret et al. 2016), that drive expression to myelomonocytic cells.[21]

Immune humanization using PBMCs and aGVHD.

In RRG animals, humanization with tissues or cells such as human skin, hepatocytes or tumor cells was possible but preliminary experiments showed that immune humanization with PBMCs was not possible.[10] To obtain immune humanization, RRG received different amounts of hPBMCs (from 230 to 1840.10^6/kg) with or without irradiation and with no other treatment. These animals did not show detectable hPBMCs in blood and they did not display any sign of aGVHD **(Table 1).** As a comparison, NSG mice receiving 300.10^6/kg hPBMCs develop aGVHD.[1,2] To obtain preliminary information on the role of rat macrophages on elimination of human cells, we treated RRG animals with liposomes containing clodronate which efficiently eliminates macrophages from organs with fenestrated endothelium, such as the spleen and liver.[20]

When RRG animals received hPBMCs (430.10^6 cells/kg) and were treated with liposomes containing clodronate and thereafter twice a week for 19 days they showed variable levels (0, 1.3, 5 and 95%, n=4) of $hCD45^+$ leukocytes in blood and spleen and in 1 out of 3 animals in the bone marrow **(Fig. 2 A, B and C).** RRG animals treated with liposomes clodronate showed early toxicity (4 out of 8 died before day 7 without weight loss or any other sign of aGVHD) **(Fig. 2 E and Table 1)** and we did not irradiate them to avoid further toxicity. Those with

hCD45+ cells (animals 3.0, 3.1 and 3.2) did not show signs of aGVHD and showed normal weight curves **(Fig. 2 E).** After withdrawal of clodronate liposome treatment during 5 weeks, leukocyte humanization was progressively lost over the 2 following weeks (from 90 to 12 %, respectively, data not shown).

All these data supported the hypothesis that immune humanization was precluded by rat macrophages.

Human SIRPa expression by rat macrophages should inhibit the phagocytosis of CD47-positive human cells by rat macrophages through delivery of "don't eat me signals". Human PBMCs (430.10^6 cells/kg) injected into RRGS animals resulted in a rapid and reproducible detection of human $CD45^+$ lymphocytes in blood, spleen, thymus and bone marrow **(Fig. 2 A, B and C).** Human $CD45^+$ leukocytes in blood were detectable at day 7 and increased by day 13. The proportion of hCD45+ cells was very high in spleen and thymus and lower in the bone marrow **(Fig. S1, SDC, http://links.lww.com/TP/B843)**. The number of hCD45+ cells in spleens at sacrifice was of 95.5 +/- 58.10^6 of cells (n=4). hCD45+ cells in blood and spleen were composed by a high proportion of T and B cells, a small fraction of NK cells and rarely of monocytes **(Fig. 2D).** T cells were composed of both CD4+ and CD8+ cells in a 2:1 ratio (data not shown). Within the first 2 weeks following hPBMC injection all RRGS consistently developed an aGVHD as shown by weight loss **(Fig. 2F)** as well as other clinical signs such as hutching, diarrhea, skin lesions, abnormal fur and reduction of locomotion **(Fig. S2, SDC, http://links.lww.com/TP/B843).**

ALT and mainly AST transaminases were elevated at 7 days and much higher at 13 days after hPBMC injection indicating hepatocyte destruction **(Fig. S3, SDC, http://links.lww.com/TP/B843).**

Injection of lower number of hPBMCs, 215.10^6 or 161.10^6 cells/kg, also resulted in aGVHD with slower kinetics and only in a small fraction of the animals when using the lowest dose in the tumor model **(data not shown and Fig. S5 [SDC, http://links.lww.com/TP/B843], respectively).**

In summary, injection of hPBMC resulted in a rapid, robust and reproducible immune humanization mainly composed of T and B cells and as a consequence in a dose-dependent acute and fatal GVHD.

aGVHD in RRGS animals as a model to apply new treatments: use of LIS1, a new porcine anti-human lymphocyte antibody.

We aimed to test a new complement-activating pig anti-human lymphocyte antibody on this RRGS model of aGVHD. To this end, we first tested in vitro the CDC capacity of the LIS1 antibody using as a source of complement rat, rabbit or human sera **(Fig. 3A)**. As comparative controls, we used mouse (NSG and C57Bl/6) sera since immunodeficient variants from these strains are the most commonly used in aGVHD models. LIS1 antibody induced the most potent CDC in the presence of rat or rabbit sera (50% CDC at ~30 □g/ml of LS1) followed by human sera (50% lysis at ~150 □g/ml). CDC was undetectable in the presence of NSG or C57Bl/6 mouse complement emphasizing the interest of RRGS vs. NSG animals **(Fig. 3A).** RRGS animals were then injected with hPBMCs and with LIS1 or control pig IgG (67p) at 40 mg/kg from day 0 and biweekly until day 28. The animals were followed for $hCD45^+$ cells in blood and clinical signs of aGVHD. All antibody control-treated RRGS animals showed rapid appearance of $hCD45^+$ cells in blood with high levels (20-50 %) at sacrifice when they reached >20% weight loss. In contrast, none of the LIS1-treated RRGS animals had detectable $hCD45R^+$ cells in the blood neither at early nor at late (day 57) time points after treatment withdrawal **(Fig. 3B)**. One LIS1-treated RRGS animal sacrificed at day 30 did not show detectable hCD45+ cells neither in the blood not in the spleen **(data not shown).** All antibody control-treated RRGS animals developed fatal aGVHD as shown by >20% weight loss before

day 17 **(Fig. 3C)** as well as all the other clinical signs **(Fig. S4, SDC, http://links.lww.com/TP/B843)** whereas all LIS1-treated RRGS animals gained weight **(Fig. 3C)** and did not have other clinical signs of aGVHD **(Fig. S4, SDC, http://links.lww.com/TP/B843)** at least until day 60.

Thus, RRGS constitute a useful model for the study of complement-activating depleting antibodies and this new anti-lymphocyte antibody is shown for the first time to be a very effective treatment of human immune responses in vivo, particularly for aGVHD.

RRGS animals as a model of cellular human anti-tumor immune responses.

To assess human immune responses against tumors in RRGS, we implanted subcutaneously a human mammal cancer cell line and when tumors were detectable (day 7) we injected human PBMCs at a dose that would not induce a rapid aGVHD ($161x10^6$ cells) and analyzed both the growth of the tumors and signs of aGVHD **(Fig. 4).** Tumor growth was inhibited in all RRGS animals only when injected with hPBMCs **(Fig. 4A).** The weight curve of RRGS animals injected or not with tumors increased with the exception of one RRGS animal treated with PBMCs that died of aGVHD at day 30 but without detectable tumor **(Fig. 4B).** This animal had a high level of $hCD45RC^+$ cells in blood (45.8 %) whereas the other animals showed low or no signs of aGVHD and survived **(Fig. S5, SDC, http://links.lww.com/TP/B843).**

Discussion.

Although immune humanized mouse models are very useful in a wide variety of models, immune humanization of immunodeficient rats have advantages in certain aspects. Rats are 10 times bigger than mice and analysis of certain models may beneficiate of this larger size, such as implantation of human tumors in small anatomical locations such as prostate and precise locations in the brain or of organoids in orthotropic locations. Inbred mouse strains have very low complement activity whereas rats have complement levels comparable to humans, as previously shown for several strains of each species[3] and in this work specifically comparing NSG and RRGS serum to obtain cytotoxicity using a new complement-activating anti-

lymphocyte antibody. Another advantage of rats is that following injection of hPBMCs and aGVHD the number of human cells obtained from a spleen of RRGS animals (50-150.10^6 cells) is much higher than those obtained from spleens of immunodeficient mice with an aGVHD (2-10.10^6 cells) (data not shown). Therefore, functional and molecular studies in subpopulations of human cells, such as Treg, during activation and aGVHD are more feasible using RRGS rather than NSG animals.

A weakness of human aGVHD models in immunodeficient mice is the use of total body irradiation to observe clear clinical GVHD, which is increasingly disparate to clinical practice, and which is not needed in this RRGS model. Additionally, *Prkdc* mutations to obtain a Scid phenotype in many mouse strains (like in all NOD-derived immunodeficient strains such as NSG and NOG) and several rat immunodeficient models[6,16] limit the use of irradiation needed in certain models such as in cancer treatments since PRKDC is an enzyme essential in DNA nonhomologous end joining and this generates uncontrolled toxicity in the host tissues. RRGS animals do not have mutations in the *Prkdc* gene and should be thus more adapted to this kind of experiments.

A series of rat immunodeficient models are available. The first of these rats and the only for many years were nude rats due to a mutation in the *Foxn1* gene.[22] Nevertheless, nude rats as nude mice are only T cell deficient, while B and NK cells are normal. Furthermore, they have a leaky phenotype that makes that older animals have T cells.[23,24] In more recent years, a series of immunodeficient rats due to mutations in other genes have been generated, including animals deficient for Rag1,[7,8] *Rag2*[25] or *Il2rg.*[26] Nevertheless, the *Rag1* and *Rag2* KO rats have normal NK cells and there is residual B and T cells for *Rag1*, *Rag2* or *Il2rg* mutated animals. More severe immunodeficient animals combining several mutations of the above mention genes have been more recently described.[6,8-10] A very recent publication with combined mutations for *Prkdc*, *Il2rg* and expression of the hSIRPa allowed better immune humanization compared to animals without hSIRPa.[16] Our results confirm the beneficial effect of hSIRPa to obtain immune

humanization and extend for the first time the use of these animals to models of aGVHD and anti-tumor immune responses.

In the RRGS aGVHD model, we confirmed the potential of a new anti-human T cell polyclonal antibody functioning through complement activation to be applied in human GVHD. The levels of complement in the large majority of inbred mouse inbred strains,[3] including NOD-derived immunodeficient animals,[14,15] is undetectable or very low. This led to the recent development of a complement sufficient NSG strain.[27] Nevertheless, NOD mice also lack NK cells[15] and are thus not suitable for analysis of ADCC mechanisms. Since LS1 antibody does not kill directly human cells in the absence of complement, the complete elimination in vivo was due to CDC and/or ADCC in proportions that need to be analyzed in the future.

Our results also show for the first time human anti-tumor immune responses allowing in the future to use RRGS animals in experiments aiming to evaluate these responses.

Immune humanization of RRGS using human CD34+ hematopoietic precursors will be the objective of new studies. Previous work with another rat line showed that this is feasible when using at the same time hCD34+ cells from fetal liver and fetal thymus but the degree of humanization was low as compared to NSG mice.[16]

The use of immunodeficient rats has limitations compared to immunodeficient mice, since their larger size implies the use of a larger space in animal facilities and thus a higher cost. Also, their larger size demands the use per body weight of larger amounts of cells or molecules to obtain the same effect.

In conclusion, RRGS animals were efficiently immune humanized using PBMCs and human aGVHD and anti-tumor immune responses could be detected. Furthermore, a new anti-lymphocyte antibody was used for the first time to inhibit in vivo human immune responses.

References

1. Walsh NC, Kenney LL, Jangalwe S, et al. Humanized Mouse Models of Clinical Disease. *Annu Rev Pathol.* 2017;12:187-215.
2. De La Rochere P, Guil-Luna S, Decaudin D, et al. Humanized Mice for the Study of Immuno-Oncology. *Trends Immunol*. 2018;39(9):748-763.
3. Ong GL, Mattes MJ. Mouse strains with typical mammalian levels of complement activity. *J Immunol Methods*.1989;125(1-2):147-158.
4. Larcher, T, Lafoux A, Tesson L, et al.Characterization of dystrophin deficient rats: a new model for Duchenne muscular dystrophy. *PLoS ONE*. 2014;9(10):e110371.
5. Wildner, G. Are rats more human than mice?. *Immunobiology*. 2019;224(1):172-176.
6. Mashimo T, Takizawa A, Kobayashi J, et al. Generation and characterization of severe combined immunodeficiency rats. *Cell Rep*. 2012;2(3):685-694.
7. Menoret S, Fontaniere S, Jantz D, et al. Generation of Rag1-knockout immunodeficient rats and mice using engineered meganucleases. *FASEB J*. 2013;27(2):703-711.
8. Tsuchida T, Zheng YW, Zhang RR, et al. The development of humanized liver with Rag1 knockout rats. *Transplant Proc*. 2014;46(4):1191-1193.
9. He D, Zhang J, Wu W, et al. A novel immunodeficient rat model supports human lung cancer xenografts. *FASEB J*. 2019;33(1):140-150.
10. Menoret S, Ouisse LH. Tesson L, et al. Generation of immunodeficient rats with Rag1 and Il2rg gene deletions and human tissue grafting models. *Transplantation*. 2018;102(8):1271-1278.
11. Legrand N, Huntington ND, Nagasawa M, et al. Functional CD47/signal regulatory protein alpha (SIRP(alpha)) interaction is required for optimal human T- and natural killer- (NK) cell homeostasis in vivo. *Proc Natl Acad Sci U.S.A*. 2011;108(32):13224-13229.

12. Strowig T, Rongvaux A, Rathinam C, et al. Transgenic expression of human signal regulatory protein alpha in Rag2-/-gamma(c)-/- mice improves engraftment of human hematopoietic cells in humanized mice. *Proc Natl Acad Sci U.S.A.* 2011;108(32):13218-13223.
13. Takenaka K, Prasolava TK, Wang JC, et al. Polymorphism in Sirpa modulates engraftment of human hematopoietic stem cells. *Nat Immuno*. 2007;8(12):1313-1323.
14. Baxter AG and Cooke A. Complement lytic activity has no role in the pathogenesis of autoimmune diabetes in NOD mice. *Diabetes.* 1993;42(11):1574-1578.
15. Shultz LD, Schweitzer PA, Christianson SW, et al. Multiple defects in innate and adaptive immunologic function in NOD/LtSz-scid mice. *J Immunol*. 1995;154(1):180-191.
16. Yang X, Zhou J, He J, et al. An Immune System-Modified Rat Model for Human Stem Cell Transplantation Research. *Stem Cell Reports*. 2018;11(2):514-521.
17. Jung CJ, Menoret S, Brusselle L, et al. Comparative Analysis of piggyBac, CRISPR/Cas9 and TALEN Mediated BAC Transgenesis in the Zygote for the Generation of Humanized SIRPA Rats. *Sci Rep.* 2016;6:31455.
18. Chenouard V, Brusselle L., Heslan JM, et al. A Rapid and Cost-Effective Method for Genotyping Genome-Edited Animals: A Heteroduplex Mobility Assay Using Microfluidic Capillary Electrophoresis. *J Genet Genomics.* 2016;43(5):341-348.
19. Menoret S, Iscache AL, Tesson L, et al. Characterization of immunoglobulin heavy chain knockout rats. *Eur J Immunol*. 2010;40(10):2932-2941.
20. Van Rooijen N, Sanders A. Liposome mediated depletion of macrophages: mechanism of action, preparation of liposomes and applications. *J Immunol Methods*. 1994;174(1-2):83-93.

21. Adams S, van der Laan LJ, Vernon-Wilson E, et al. Signal-regulatory protein is selectively expressed by myeloid and neuronal cells. *J Immunol.* 1998;161(4):1853-1859.

22. Festing MF, May D, Connors TA, et al. An athymic nude mutation in the rat. *Nature.* 1978;274(5669):365-366.

23. Colston MJ, Fieldsteel AH and Dawson PJ. Growth and regression of human tumor cell lines in congenitally athymic (rnu/rnu) rats. *J Natl Cancer Inst*. 1981;66(5):843-848.

24. Vaessen LM, Broekhuizen R, Rozing J, et al. T-cell development during ageing in congenitally athymic (nude) rats. *Scand J Immuno*l. 1986;24(2):223-235.

25. Noto FK, Adjan-Steffey V, Tong M, et al. Sprague Dawley Rag2-Null Rats Created from Engineered Spermatogonial Stem Cells Are Immunodeficient and Permissive to Human Xenografts. *Mol Cancer Ther*. 2018;17(11):2481-2489.

26. Mashimo T, Takizawa A, Voigt B, et al. Generation of knockout rats with X-linked severe combined immunodeficiency (X-SCID) using zinc-finger nucleases. *PLoS One.* 2010;5(1):e8870.

27. Verma MK, Clemens J, Burzenski L, et al. A novel hemolytic complement-sufficient NSG mouse model supports studies of complement-mediated antitumor activity in vivo. *J Immunol Methods.* 2017;446:47-53.

Figure Legends.

Figure 1. Cytometry analysis of rat leukocytes and hSIRPa expression in RRGS animals. PBMCs from spleen and bone marrow were collected from WT and RRGS animals and stained with the indicated antibodies and with hCD47Fc. **A)** Representative dot plots of T, NK and B cells in the spleen of one RRGS animal. Numbers within dot plots represent percentage of positive cells. **B)** Mean proportion in the spleen of T, NK and B cells +/- SD of n=4 RRGS animals analyzed. **C)** Representative dot plots of T, NK and B cells in the bone marrow of one RRGS animal. Numbers within dot plots represent percentage of positive cells. **D)** Representative dot plot rat CD11b+ cells labeled with anti-rat and anti-human SIRPa mAbs as well as with hCD47 and anti-hSIRPa in WT and RRGS animals**.** Numbers within dot plots represent percentage of positive cells. **E)** Mean proportion among rat CD11b+ cells of rat SIRPa+ and human SIRPa+ cells as well as of hCD47+ and human SIRPa+ cells in 4 RRGS and 4 WT animals analyzed.

Figure 2. aGVHD in RRGS animals injected with hPBMCs. hPBMCs from healthy volunteers were injected iv ($430x10^6$ cells/kg) in RRG, RRGS or WT animals. RRG animals received or not treatment with liposomes clodronate. **A)** Representative dot plots of blood performed after hPBMC injection for detection of rat and human $CD45^+$ cells. Numbers within dot plots represent percentage of positive cells. **B)** Upper. Mean +/- SD proportion of hCD45+ cells in blood of RRGS animals (n=4). Lower. Mean +/- SD proportion of hCD45+ cells in blood of RRG animals with (n=8) or without (n=2) liposomes clodronate. **C)** Representative dot plots of hCD45+ cells in spleen, thymus and bone marrow at sacrifice (day 17 and 19 after PBMC injection for RRGS and RRG, respectively). Numbers within dot plots represent percentage of positive cells. **D)** Subset composition of $hCD45^+$ cells in blood and spleen of an RRGS animal sacrificed at day 17 after hPBMCs injection. CD3 for T cells, CD19 for B cells, CD56 for NK cells and CD14 for monocytes. **E)** Weight curves of RRG animals injected or not with hPBMCs and with or without liposomes clodronate. †: animals that died spontaneously

without any signs of aGVHD. **F)** Weight curves of RRGS animals injected or not with hPBMCs. †: sacrificed animals when weight loss and other clinical signs showed irreversible aGVHD.

Figure 3. Evaluation of a new anti-lymphocyte antibody (LIS1) for the treatment of aGVHD in RRGS animals. A) Evaluation of CDC using hPBMCs was performed by in vitro incubation with pure rat, human, NSG C57/Bl6 serum as source of complement and increasing doses of purified pig LS1 or control nonimmune (67p) IgG (n=3 donors for each serum species used in 3 independent experiments). **B)** hPBMCs from healthy volunteers were injected iv ($215x10^6$ cells/kg) to RRGS animals treated with LIS1 or control IgG (67p) injected from the day of hPBMC injection biweekly until day 28. Proportion of $hCD45^+$ cells in blood at different time points on LIS1 or control IgG (67p)-treated RRGS. **C)** Weight curves of LIS1 or control IgG (67p)-treated RRGS. †: sacrificed animals due to >20% weight loss. ✸ sacrificed animal for analysis of $hCD45^+$ cells.

Figure 4. Tumor model and anti-tumor immune response using hPBMCs. Human mammary tumor cells (B2 cell line) were injected subcutaneously in RRGS animals (n=8) and when tumors were measurable (day 0), RRGS animals were injected iv with hPBMCs ($161x10^6$ cells/kg, n=4) or PBS (n=4). **A)** Tumor volume were determined at the indicated time points in RRGS animals injected or not with hPBMCs. **B)** Weight curves of RRGS animals injected or not with hPBMCs. †: sacrificed animal due to weight loss >20%.

Supplementary figure legends.

Figure S1: Analysis of the proportion of hCD45+ cells in RRGS animals immune humanized with hPBMCs. RRGS or WT animals (n=5 each) were injected iv with hPBMCs (430.10^6 cells/Kg) from healthy volunteers and sacrificed at day 13 after hPBMCs infusion. hCD45+ cells were analyzed in the indicated organs.

Figure S2. aGVHD clinical score of RRGS animals injected with hPBMCs. hPBMCs (430.106 cells/Kg) from healthy volunteers were injected iv in RRGS or WT animals. Different clinical parameters; hutching, rough fur, skin lesions, decreased physical activity, diarrhea, and weight loss were scored as 0=no signs, 1=present. WT+hPBMCs, n=5. RRGS+hPBMCs, n=5.

Figure S3. Alanine and aspartate transaminases (ALT and AST) in serum during aGVHD in RRGS animals. hPBMCs (430.106 cells/Kg) from healthy volunteers were injected iv in RRGS or WT animals and serum was harvested at the indicated time points for analysis of AST and ALT. WT+hPBMCs, n=5. RRGS+hPBMCs, n=5.

Figure S4. aGVHD clinical score of RRGS animals injected with hPBMCs treated or not with LIS1. hPBMCs from healthy volunteers were injected iv (215.10^6 cells/Kg) in RRGS animals treated or not with LIS1 or 67p (antibody control). Different clinical parameters; hutching, rough fur, skin lesions, decreased physical activity, diarrhea, and weight loss were scored as 0=no signs, 1=present. RRGS+hPBMCs+67p, n=5. RRGS+hPBMCs+LIS1, n=5.

Figure S5. aGVHD clinical score of RRGS animals injected with hPBMCs and tumors. RRGS animals were injected with a human tumor cell line (B2 cells line) and then injected or not with hPBMCs iv (161.10^6 cells/Kg). Different clinical parameters; hutching, rough fur, skin lesions, decreased physical activity, diarrhea, and weight loss were scored as 0=no signs, 1=present. RRGS+ tumor cells, n=4. RRGS+ tumor cells + hPBMC, n=4. One out of 4 RRGS+hPBMC animals developed aGVHD.

Table 1.

Age (weeks)	hPBMC/kg	Number of rats	Macrophage depletion	Irradiation (2Gy)	hPBMC detection with liposomes clodronate (LC)	GVHD
8	230.10^6 /kg	2	No	No	No	No GVHD
8	460.10^6 /kg	2	No	No	No	No GVHD
8	690.10^6 /kg	2	No	No	No	No GVHD
8	1150.10^6 /kg	2	No	No	No	No GVHD
8	1840.10^6 /kg	1	No	No	No	No GVHD
8	1150.10^6 /kg	4	No	Yes	No	No GVHD
8	1840.10^6 /kg	2	No	Yes	No	No GVHD
8	1150.10^6 /kg	1	Yes	No	No	No GVHD
4	430. 10^6/kg	6 : 1 w/o hPBMC 5 hPBMC +LC	Yes 4 rats died in the LC group	No	Yes in hPBMC+LC group (1 out of 2) D20 : 14.3%	No GVHD
4	430. 10^6/kg	11 :	Yes	No	Yes in hPBMC+LC group	No GVHD

		1 w/o hPBMC 2 hPBMC 8 hPBMC + LC	4 rats died in the LC group		(3 out of 4) D19 : 30.3% (SD 41.8%)	
4	430. 10^6/kg	8 : 2 CL w/o hPBMC 2 hPBMC 4 hPBMC+ LC	Yes	No	Yes in hPBMC+LC group (3 out of 4) D5 : 1.4% (SD 1.4%)	No GVHD

Figure 1.

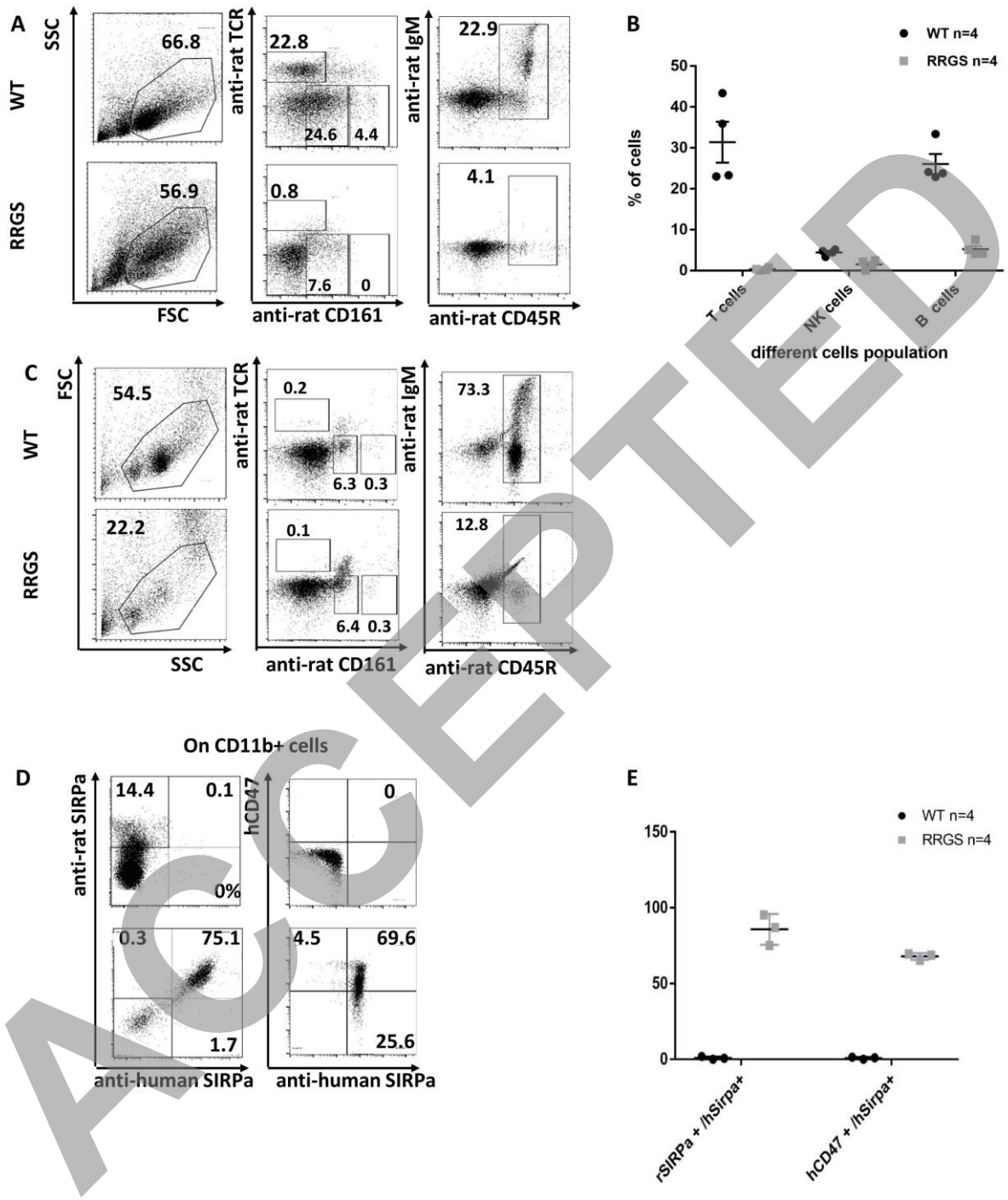

Figure 2.

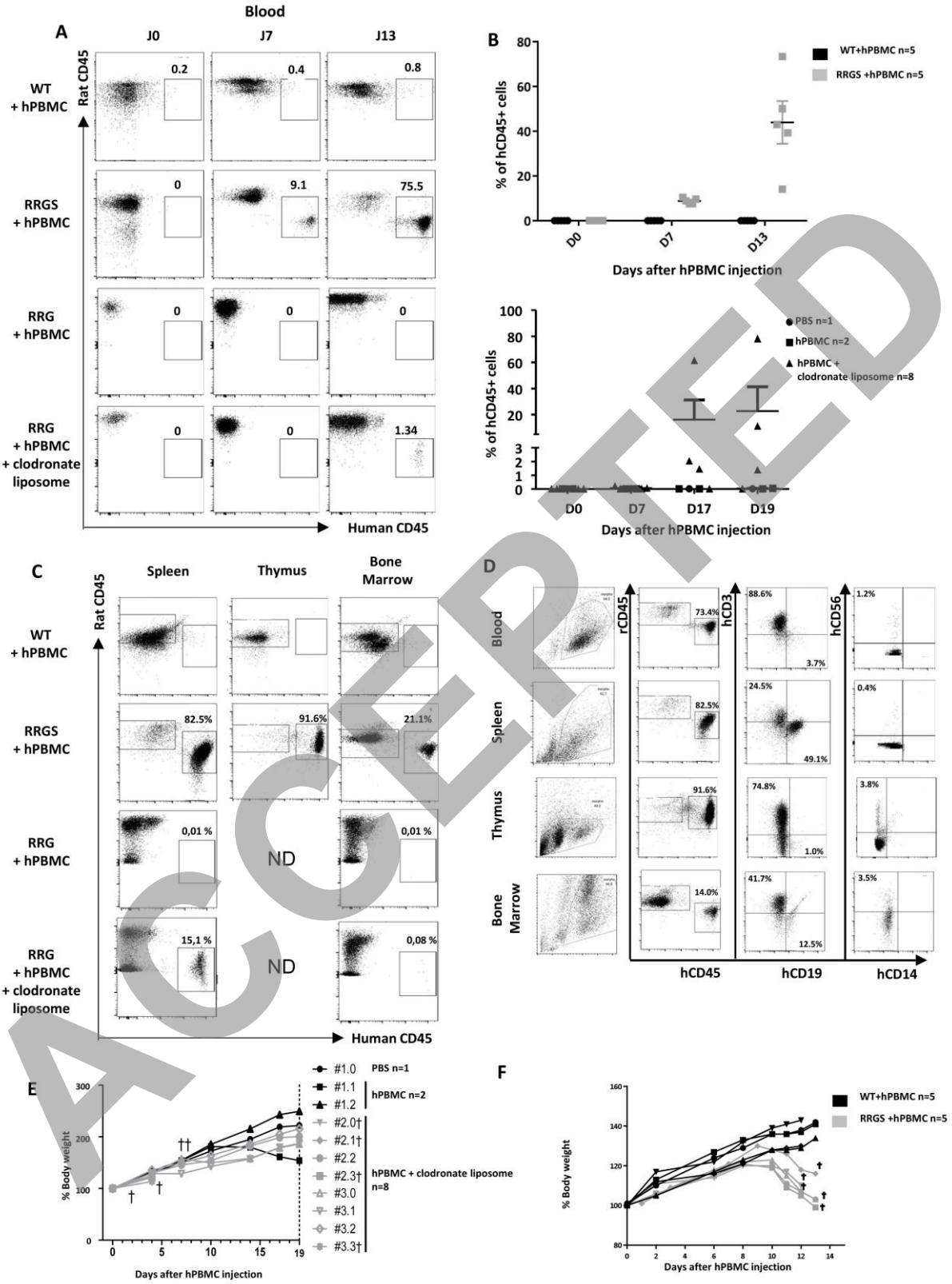

Figure 3.

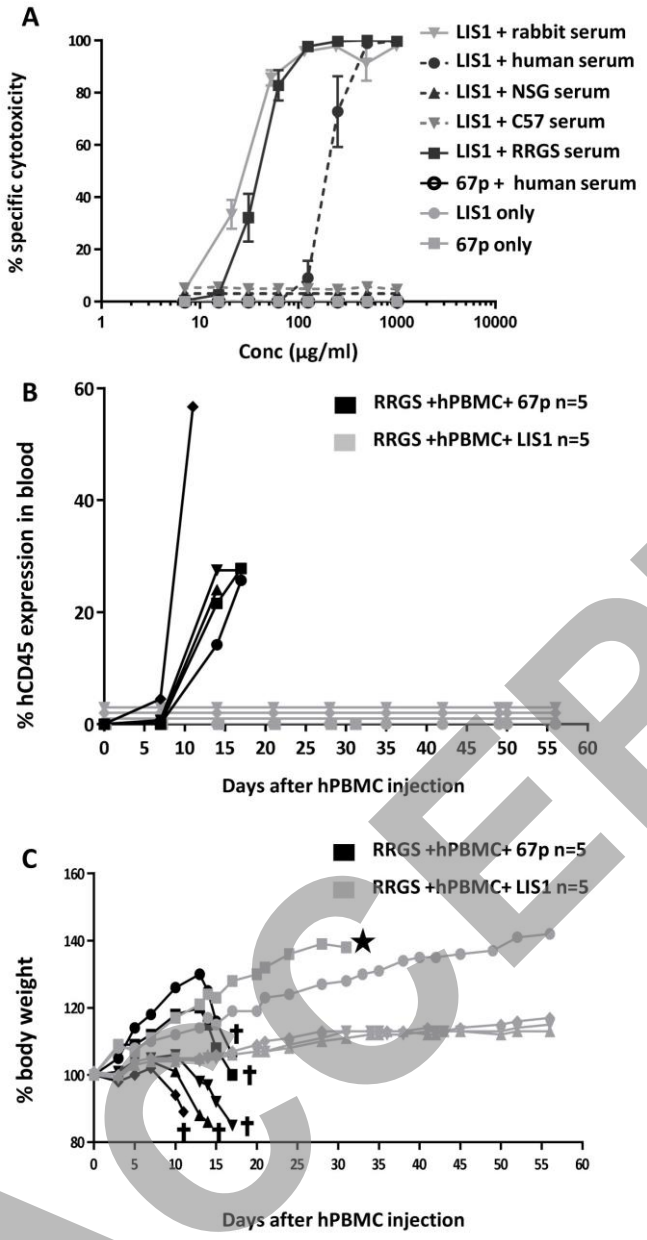

Figure 4.